

The role of total pressure in gas-phase nucleation: A diffusion effect

S.-M. Suh and S. L. Girshick

Department of Mechanical Engineering, University of Minnesota, Minneapolis, Minnesota 55455

M. R. Zachariah^{a)}

Department of Mechanical Engineering and Department of Chemistry, University of Minnesota, Minneapolis, Minnesota 55455

(Received 17 January 2002; accepted 10 May 2002)

A numerical modeling study is presented concerning the role of total pressure in gas-phase nucleation. We consider a generic self-clustering mechanism for particle production in which the cluster transport properties are assumed to scale with monomer properties. A steady-state isothermal plug flow reactor model is considered in which axial diffusion of gas species is allowed. Species conservation equations with appropriate boundary conditions are solved in the one-dimensional reactor space. A steady-state nucleation current is shown to be achievable when the monomer concentration is fixed, regardless of the total pressure. In the case when the monomer concentration is varied, we demonstrate that diffusion can play a critical role at low pressures, where the nucleation rate is found to be highly pressure-sensitive. In this regime steady-state nucleation is not possible. As pressure increases, the nucleation rate becomes gradually pressure-insensitive and approaches the high-pressure limit. A dimensionless analysis is performed for a series of irreversible clustering reactions, and the effects of dimensionless system parameters on the nucleation rate are presented as a function of pressure. The results indicate that to minimize particle formation in chemical vapor deposition reactors while maintaining high deposition rates one should operate in the pressure-dependent regime, with low total reactor pressures and high partial pressures of reactants. © 2003 American Institute of Physics. [DOI: 10.1063/1.1490345]

NOMENCLATURE

A	Reactant
A_1	Constant
A_2	Constant
B	Reactant
C_{ref}	Reference concentration
$C_{A,0}$	Inlet reactant concentration as defined in Table I
C_i	Concentration of the i -mer
$C'_{A,0}$	Dimensionless inlet reactant concentration as defined in Table I
D_i	Diffusion coefficient of the i -mer
D'_a	Damkohler number as defined in Table I
G_i	i -mer
J_i	Nucleation current where the i -mer is produced
J'	Normalized nucleation rate as defined in Table I
k_i	Forward rate constant of the reaction that forms the i -mer
k_{-i}	Reverse rate constant of the reaction that forms the i -mer
L	Reactor length
P'	Dimensionless pressure parameter as defined in Table I
p	Pressure
R'	Dimensionless reaction rate parameter as defined in Table I
R'^{-1}	Reciprocal of R' as defined in Table I

t	Time
u	Axial velocity
x	Axial distance
x'	Dimensionless axial distance
α	Multiplicative factor to the base case k_{-i}
β	Multiplicative factor to the base case C_1
γ	Multiplicative factor to the base case k_1

I. INTRODUCTION

Considerable research has been performed both theoretically and experimentally to understand gas phase nucleation phenomena which lead to particle formation. Recently attention has been paid to understanding particle contamination during chemical vapor deposition (CVD) of semiconductor materials in which gas-phase nucleation is considered to be primarily responsible for the generation of particles with sizes on the order of tens of nanometers. It is interesting to note that, during the CVD processes, total gas pressure has been reported to play a significant role in particle production. These observed pressure effects may result from entirely different physical-chemical phenomena depending on the chemistry and the configuration of the system.¹⁻⁴

For example, in low-pressure CVD of silicon from thermally activated silane, the observed dependence of particle production on pressure has been attributed to the competition between third-body stabilization and the decomposition of key growth species.^{1,2} A strong pressure dependence has also been observed for particle production during silane oxidation.^{3,4} This latter observation was explained⁵ by the

^{a)} Author to whom correspondence should be addressed. Telephone: 613-626-9081; Electronic mail: mrz@me.umn.edu

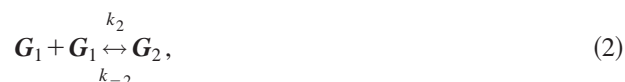
combined synergistic effects of several system parameters that are associated with the pressure change, including flow residence time, partial pressure change, and diffusional loss of highly reactive radicals that initiate the chain-branching silane oxidation chemistry.

In homogeneous nucleation theory, the presence of a rate-limiting bottleneck in a clustering sequence leads to the establishment of a steady-state nucleation current, provided that there is an ample supply of monomers. In this study, we explore the potentially important role of cluster diffusion in particle formation, in a regime where the steady-state nucleation current assumption cannot hold due to the variation in monomer concentration, and consequently total pressure can have a considerable impact.

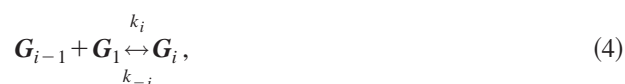
A description of the numerical model is presented in Sec. II. A generic self-clustering mechanism for particle production is considered for a steady-state isothermal plug-flow reactor with axial diffusion of gas species. In Sec. III we consider the conditions for validity of the steady-state nucleation assumption, followed in Sec. IV by a dimensionless analysis that assumes an irreversible clustering sequence. A dimensionless set of species conservation equations with appropriate boundary conditions is solved for a one-dimensional reactor space. The pressure sensitivity of the calculated nucleation rates is investigated by varying system parameters expressed in dimensionless forms. In Sec. V a nucleation barrier is assumed in the clustering sequence, causing reactions below the barrier to be reversible. Simulations are conducted both for the case where the monomer concentration is kept spatially uniform and for the case where the monomer concentration is allowed to vary.

II. MODEL DESCRIPTION

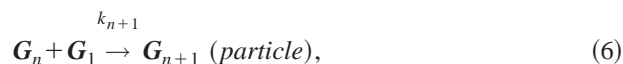
The system considered here is an isothermal, isobaric, plug-flow reactor with length L . In the base case, the monomer, denoted G_1 , is produced by reaction (1). Two reactants, A and B , and a carrier gas, D , are introduced at a constant inlet velocity, u . The concentration of the carrier gas is adjusted to maintain a specified total gas pressure, while the reactant concentrations are kept constant throughout the pressure change. Clustering is assumed to occur by the addition–abstraction of monomers, as expressed in reactions (2)–(6):



≈



≈



where k_i and k_{-i} are, respectively, the forward and reverse rate constants of the monomer addition reaction that forms an i -mer. “Particles” are formed irreversibly at the last step, given by reaction (6). By adjusting the reverse rate constants for the clustering sequence in reactions (2)–(6), a nucleation barrier can be inserted at a certain step, forming a critical cluster, below which clusters tend to shrink and above which cluster growth is effectively irreversible.

The steady-state (time-independent) gas species mass conservation equations can be written as follows:

$$A \text{ or } B: \quad u \frac{dC_A}{dx} - D_A \frac{d^2C_A}{dx^2} = -k_1 C_A C_B, \tag{7}$$

$$G_1: \quad u \frac{dC_1}{dx} - D_1 \frac{d^2C_1}{dx^2} = k_1 C_A C_B - \sum_{j=2}^{n+1} J_j, \tag{8}$$

$$G_i, \text{ for } 2 \leq i \leq n: \quad u \frac{dC_i}{dx} - D_i \frac{d^2C_i}{dx^2} = J_i - J_{i+1}, \tag{9}$$

$$G_{n+1} \text{ (particle)}: \quad u \frac{dC_{n+1}}{dx} - D_{n+1} \frac{d^2C_{n+1}}{dx^2} = J_{n+1}, \tag{10}$$

where C_i and D_i represent, respectively, the concentration and the diffusion coefficient of the i -mer, G_i . J_i , the nucleation current, is the net rate of the i th reaction where the i -mer is produced as expressed in reaction (4), and takes the form

$$J_i = k_i C_{i-1} C_1 - k_{-i} C_i \quad (2 \leq i \leq n). \tag{11}$$

We take the nucleation rate to be given by the production rate of “particles,” given by

$$J_{n+1} = k_{n+1} C_n C_1. \tag{12}$$

Reactant concentrations are assumed to be given at the inlet, and a zero-gradient boundary condition is applied to the reactor exit. For simplicity we assume that the inlet concentrations of the reactants are equal to each other

$$C_A = C_B = C_{A,0} \quad \text{at } x=0, \tag{13}$$

$$\frac{dC_i}{dx} = 0, \quad \text{for all species at } x=L. \tag{14}$$

III. THE STEADY-STATE NUCLEATION ASSUMPTION AND ITS VALIDITY FOR A SYSTEM WITH DIFFUSION

Equations (7)–(14) are written for a system that is time-independent and varies only in the x -direction. However, as the flow points in the x direction, one can also interpret x as a time variable, representing time as experienced by a parcel of fluid traveling with the bulk flow. The zero-gradient boundary condition for species concentrations at $x=L$ can

thus be interpreted as representing a sufficiently long time, at which species concentrations are no longer changing.

If instead one considered a closed system that is spatially uniform (hence, without any transport effects) but varying in time, the rates of change of the cluster concentrations would be given by

$$\frac{dC_i}{dt} = J_i - J_{i+1} \quad (2 \leq i \leq n). \quad (15)$$

In that case, if steady state prevailed, the nucleation currents would all be instantaneously equal to each other

$$J_2 = J_3 = \dots = J_{n+1}. \quad (16)$$

In many cases, even for open systems with transport and rapidly changing conditions, the existence of steady state nucleation has been shown to be a reasonable approximation. We here use our simple plug flow model to examine the conditions of validity for the steady-state nucleation approximation, which we take to be defined by Eq. (16).

If steady-state nucleation holds, then Eq. (9) can be rewritten

$$u \frac{dC_i}{dx} - D_i \frac{d^2 C_i}{dx^2} = 0. \quad (17)$$

The solution of the above differential equation takes the following form:

$$C_i = A_1 e^{ux/D_i} + A_2, \quad (18)$$

where A_1 and A_2 are constants to be determined from the boundary conditions. After applying the downstream boundary condition of Eqs. (14)–(18), one obtains

$$C_i = \text{constant}, \quad \text{for } 2 \leq i \leq n. \quad (19)$$

On the other hand, from $J_2 = J_3$, equating $J_2 = k_2 C_1^2 - k_{-2} C_2$ and $J_3 = k_3 C_2 C_1 - k_{-3} C_3$, and solving for C_1 yields

$$C_1 = \frac{k_3 C_2 \pm \sqrt{(k_3 C_2)^2 - 4k_2(k_{-3} C_3 - k_{-2} C_2)}}{2k_2}. \quad (20)$$

From Eq. (19) C_2 and C_3 are constant. Therefore, as the rate constants, k_2 , k_{-2} , k_3 , and k_{-3} , do not vary spatially in this isothermal system, one can deduce from Eq. (20) that

$$C_1 = \text{constant}. \quad (21)$$

Thus, for the steady-state nucleation current, $J_2 = J_3 = \dots = J_{n+1}$, to be established, it is necessary that the monomer concentration be held constant. In this case, species transport has no role to play, because $dC_i/dx = d^2 C_i/dx^2 = 0$ from Eqs. (19) and (21).

In the case where the monomer concentration varies due either to reactant depletion or to a change in reaction kinetics, caused, for example, by a temperature gradient inside the reactor, the nucleation current at each step becomes different by the amount of the two transport terms in Eq. (9). In particular, for the case where diffusion dominates convection ($uL/D_i \ll 1$), or in the downstream region of the reactor where species concentration profiles effectively flatten out (i.e., $dC_i/dx \approx 0$), the convection term becomes relatively negligible and the following relationship holds:

$$J_i - J_{i+1} = -D_i \frac{d^2 C_i}{dx^2}, \quad \text{for } 2 \leq i \leq n. \quad (22)$$

In summary, one can conclude the following from the analysis presented in this section:

- If $J_2 = J_3 = \dots = J_{n+1}$, then $C_i = \text{constant}$ for $1 \leq i \leq n$;
- the steady-state nucleation current assumption cannot hold in the case where the monomer concentration varies and cluster diffusion is important.

IV. IRREVERSIBLE CLUSTERING

As a limiting case, the reverse rate constants, k_{-i} in reactions (2)–(5), are all set to be zero and a series of irreversible clustering reactions is considered in this section. This allows the governing equations to be cast into a simpler form, and a dimensionless analysis is performed to explain the role of total pressure in gas phase nucleation.

A. Dimensionless governing equations

Table I summarizes the general definitions and physical interpretations of the dimensionless quantities adopted. Using the dimensionless quantities together with the dimensionless axial distance, $x' = x/L$, the species conservation equations in (7)–(10) can be transformed as follows:

$$A \text{ or } B: \quad \frac{1}{D'_a} \cdot \frac{dC'_A}{dx'} = \frac{1}{P'_A} \cdot \frac{d^2 C'_A}{dx'^2} - \frac{1}{R'} \cdot C'_A C'_B, \quad (23)$$

$$G_1: \quad \frac{1}{D'_a} \cdot \frac{dC'_1}{dx'} = \frac{1}{P'_1} \cdot \frac{d^2 C'_1}{dx'^2} + \frac{1}{R'} \cdot C'_A C'_B - C'_1 (C'_1 + C'_2 + \dots + C'_n), \quad (24)$$

$$G_i, \text{ for } 2 \leq i \leq n: \quad \frac{1}{D'_a} \cdot \frac{dC'_i}{dx'} = \frac{1}{P'_i} \cdot \frac{d^2 C'_i}{dx'^2} + C'_1 (C'_{i-1} - C'_i), \quad (25)$$

$$\text{particle:} \quad \frac{1}{D'_a} \cdot \frac{dC'_{\text{particle}}}{dx'} = \frac{1}{P'_{\text{particle}}} \cdot \frac{d^2 C'_{\text{particle}}}{dx'^2} + C'_1 C'_n, \quad (26)$$

where the Damkohler number, D'_a , and the dimensionless reaction rate parameter, R' , are defined, respectively, as $D'_a = k_2 C_{\text{ref}}/uL$ and $R' = k_2/k_1$, and where C_{ref} is a reference concentration, arbitrarily set equal to 10^{14} cm^{-3} . In defining R' , all the polymerization rate constants, k_i (for $2 \leq i \leq n$), are set equal to k_2 for simplicity. P' is referred to as the dimensionless pressure (or diffusion) parameter of the i -mer, and defined as $P' = k_2 C_{\text{ref}}/D_i/L^2$. The interpretation of P'_i as a pressure term arises from the dependence of the diffusion coefficient on pressure. In a dilute system, species diffusion parameters can be simplified by ignoring the differences in transport properties among A , B , C , D , and P_1 compared to those of larger clusters. Thus $P'_A \cong P'_B \cong P'_D \cong P'_1 \cong P'$. Moreover, as we arbitrarily assume that the mass and the collision diameter of the i -mer are i times those of the monomer, one obtains $P'_i = \sqrt{i}(i+1)^2 P'$ after manipulating the binary diffusion coefficient of the i -mer.

TABLE I. Dimensionless quantities and physical interpretation.

Dimensionless quantities	Physical interpretation ^a
$P' = \frac{k_2 C_{\text{ref}}}{D_1 / L^2} \equiv \frac{\text{Polymerization rate}}{\text{Diffusion rate}^b}$	$P' \propto \text{pressure}$
$R' = \frac{k_2}{k_1} \equiv \frac{\text{Polymerization rate constant}}{\text{Monomer production rate constant}}$	$R'^{-1} = \frac{1}{R'} \propto \text{monomer product}$
$D'_a = \frac{k_2 C_{\text{ref}}}{u/L} \equiv \frac{\text{Polymerization rate}}{\text{Convective transport rate}}$	$D'_a \propto \text{residence time}$
$C'_{A,0} = \frac{C_{A,0}}{C_{\text{ref}}} \equiv \frac{\text{Inlet reactant concentration}}{\text{Reference concentration}^c}$	$C'_{A,0} \propto \text{precursor concentration}$
$C'_k = \frac{C_k}{C_{\text{ref}}} \equiv \frac{k\text{-mer concentration}}{\text{Reference concentration}^c}$	
$J' = \frac{J}{J_{\text{ref}}} \equiv \frac{\text{Nucleation rate}}{\text{Reference nucleation rate}^d}$	

^aAssuming that the other dimensionless quantities are fixed.

^b D_1 is the diffusion coefficient of the monomer.

^c C_{ref} is the reference concentration, which is arbitrarily chosen to be 10^{14} cm^{-3} for all the calculations.

^d J_{ref} is the reference nucleation rate, which is arbitrarily chosen to be the smallest value obtained throughout the calculation.

The boundary conditions now take the following dimensionless form:

$$C'_A = C'_B = C'_{A,0}, \quad \text{at } x' = 0, \quad (27)$$

$$\frac{dC'_k}{dx'} = 0, \quad \text{for all species at } x' = 1, \quad (28)$$

where $C'_{A,0} = C_{A,0}/C_{\text{ref}}$ and $C'_k = C_k/C_{\text{ref}}$.

B. Simulation results and discussion

The irreversible clustering model presented in the previous section was implemented by modifying the computer program PREMIX,⁶ which is one of the CHEMKIN application codes.⁷ To characterize the effect of diffusion (or pressure) in the limit of zero diffusion we solve the kinetic model utilizing SENKIN⁸ to obtain high-pressure limits in a homogeneous system, where the diffusion terms in Eqs. (23)–(26) drop out and the results become pressure-independent if initial reactant concentrations are fixed.

In this calculation, we use five clustering steps ($n = 5$) in the clustering sequence given in reactions (1)–(6) and take the production rate of G_6 as the nucleation rate. The nucleation rates are normalized by the smallest value calculated.

Figure 1 shows the normalized nucleation rate, J' , as a function of the pressure parameter, P' , for the base case condition of $R'^{-1} = 10^{-4}$, $D'_a = 166$, and $C'_{A,0} = 1$. In referring to P' we remind the reader that we refer to this term as a pressure parameter, because of the inverse pressure dependence of the diffusion coefficient (see Table I). Although the other parameters including the reactant concentrations are kept constant, it is seen that the nucleation rate increases by eight orders of magnitude with two orders of magnitude pressure increase. This is in contrast to the conventional wisdom that total pressure is unimportant in nucleation (excluding energy transfer effects). A “high-pressure” limit is achieved at around $P' = 10^3$ for this case, after which the

nucleation rate is relatively independent of pressure. The absolute magnitude of J' at the high-pressure limit is determined by the other dimensionless quantities, $C'_{A,0}$, R'^{-1} and D'_a , which are also functions of kinetic parameters as defined in Table I. Therefore, the pressure-insensitive regime can be considered to be kinetics-controlled, while the pressure-sensitive regime is diffusion-controlled.

The effects of diffusion on the nucleation rate are two-fold: (1) Diffusion reduces the concentrations of clustering species, and the cluster production rate is nominally proportional to species concentration squared; and (2) the nucleation rate is affected by all the clustering steps sequentially, as seen in Eqs. (23)–(26). This explains the exponential dependence of the nucleation rate on pressure at lower pressures. The high-pressure limit indicated in Fig. 1, therefore,

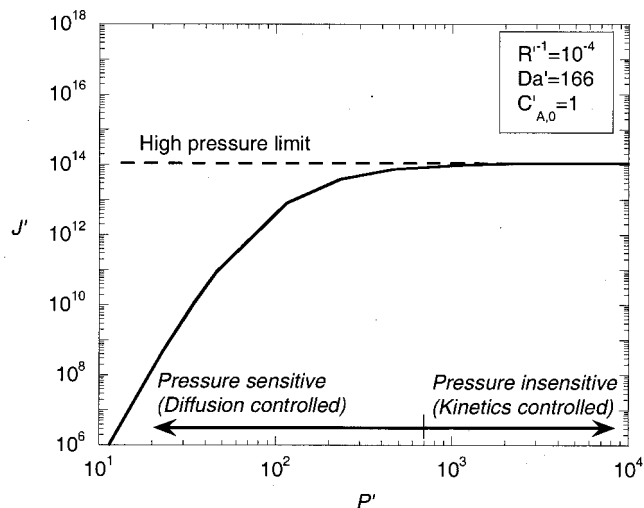


FIG. 1. Pressure sensitivity of the nucleation rate for a series of irreversible clustering reactions.

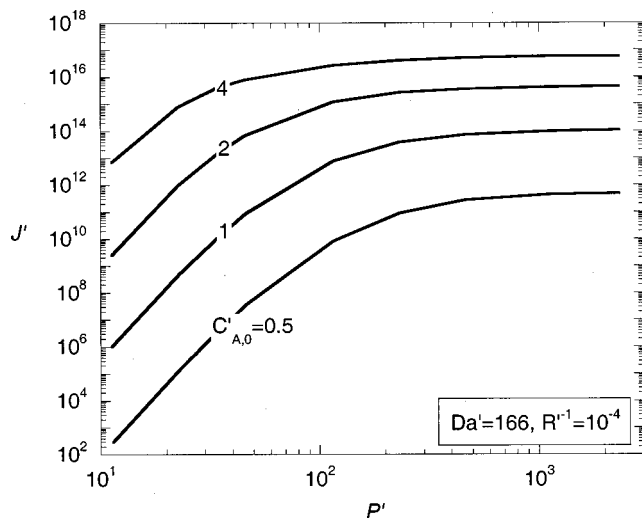


FIG. 2. The effect of the inlet reactant concentration on the nucleation rate for a series of irreversible clustering reactions.

demarks conditions where diffusive transport is important and should not be misconstrued with the high-pressure limit terminology used when referring to individual nucleation steps.^{9,10} If more clustering steps had been considered, at greater computational expense, then the nucleation rate would appear to be even more sensitive to pressure due to the contribution from each additional step.

The effect of varying inlet reactant concentrations is shown in Fig. 2. As $C'_{A,0}$ doubles, the nucleation rate increases by factors of $\sim 10^3$ – 10^4 at low pressures. The pressure sensitivity is seen to decrease at higher inlet reactant concentrations, i.e., the change in J' decreases from a factor of $\sim 10^9$ to $\sim 10^4$ when $C'_{A,0}$ is increased by a factor of eight. The decrease in the J' increment in the high-pressure limit is largely attributable to reactant depletion. In other words, since the reactant destruction rate is proportional to the concentration squared, reactant depletion is accelerated at higher $C'_{A,0}$. We also see that the pressure-insensitive regime begins at lower pressures for the higher $C'_{A,0}$ cases, which results from the fact that the chemical production terms become more important, compared to the diffusion term, at higher values of $C'_{A,0}$.

Figure 3 shows the effect of the reaction rate parameter, R' , on the nucleation rate. To keep the other dimensionless quantities constant while varying R' only the monomer production rate constant, k_1 , was changed. Interpretation of the results is made easier using R'^{-1} , the reciprocal of R' , as it is proportional to k_1 . We observe that, as R'^{-1} is increased by one order of magnitude, the nucleation rate increases by a factor of $\sim 10^6$ at low pressures. We also observe that the pressure sensitivity of the nucleation rate decreases at higher values of R'^{-1} , i.e., at higher monomer production rates, in that the change in J' over the entire pressure range considered is a factor of $\sim 10^4$ and $\sim 10^9$ when R'^{-1} equals 10^{-3} and 10^{-5} , respectively. This is due to increased reactant depletion at higher monomer production rates in the pressure-insensitive regime. In the absence of species depletion, the increment of J' due to an order of magnitude increase of R'^{-1} would be approximately a factor of 10^6 : The

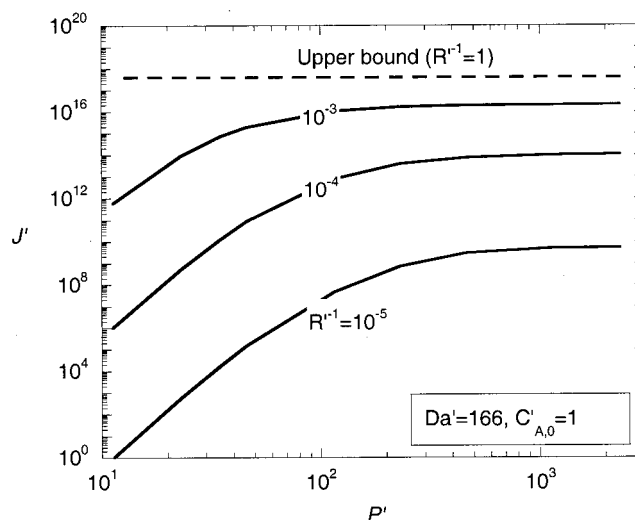


FIG. 3. The effect of the reaction rate parameter on the nucleation rate for a series of irreversible clustering reactions.

expected relative increase in monomer concentration being the same as that in R'^{-1} , raised by a power equal to the total number of monomer addition reactions (six) in the clustering sequence. As in Fig. 2, the pressure-insensitive regime is reached earlier when the chemical production term is larger, i.e., with larger R'^{-1} . As R'^{-1} approaches unity ($k_1 = k_2$), the nucleation rate approaches the “high-pressure limit,” which is virtually pressure-insensitive because the chemical production term dominates the diffusion term at all pressures.

The effect on the nucleation rate of varying the Damkohler number, D'_a , which we have defined as the ratio of the polymerization rate to the convective transport rate, is shown in Fig. 4. Changes in D'_a probe the effect of residence time through the convective velocity, u . As expected, the nucleation rate increases with increasing D'_a , as a longer time is available for clustering. However, the effect is rela-

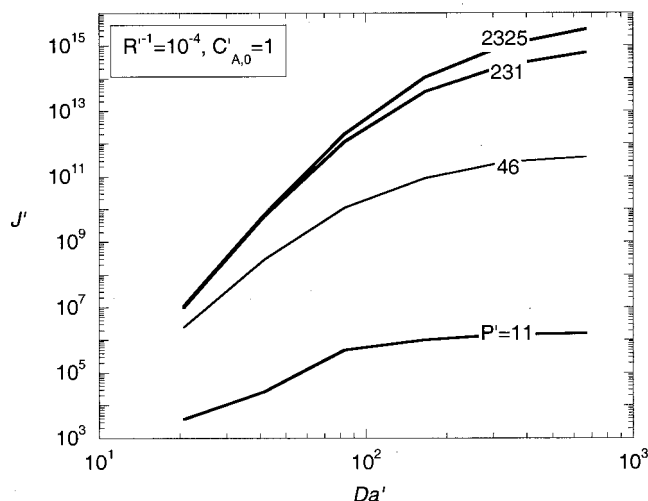


FIG. 4. The effect of Damkohler number on the nucleation rate for a series of irreversible clustering reactions.

TABLE II. Model parameters used for reversible clustering in the base case.

Model parameters	Description	Assumed values
k_1 ($\text{cm}^3 \text{mol}^{-1} \text{s}^{-1}$)	Forward rate constant for the reaction $A + B \xrightarrow{k_1} G_1 + C$	10^{10}
k_i ($\text{cm}^3 \text{mol}^{-1} \text{s}^{-1}$)	Forward rate constant for the reaction $G_{i-1} + G_1 \xrightleftharpoons[k_{-i}]{k_i} G_i$	10^{13} , for $2 \leq i \leq 6$
k_{-i} (s^{-1})	Reverse rate constant for the reaction $G_{i-1} + G_1 \xrightleftharpoons[k_{-i}]{k_i} G_i$	$(5-i) \times 10^7$, for $2 \leq i \leq 4$ 10^0 , for $i=5$ 0, for $i=6$
W_i (amu)	Molecular weight of the i -mer	$i \times 60$, for $1 \leq i \leq 6$
d_i (\AA)	Collision diameter of the i -mer	$i \times 2$, for $1 \leq i \leq 6$
p	Pressure	$0.1 - 10^3$ Torr ($1.33 \times 10^1 - 1.33 \times 10^5$ Pa)
T	Temperature	300 K
C_1	Monomer concentration in the case when held constant	$1 \times 10^{16} \text{cm}^{-3}$
C_A, C_B	Reactant concentration	$1.7 \times 10^{15} \text{cm}^{-3}$

tively small at low pressures, when the diffusive velocity is greater than the convective velocity (i.e., $P'/D'_a < 1$). The variation of the nucleation rate gradually decreases with respect to pressure, and no significant difference is observed when P' is changed from 231 to 2325. This is similar to the effect observed in Fig. 3, i.e., particle production becomes reactant-concentration controlled at high P' . Overall, the nucleation rate is found to be less pressure-sensitive at lower D'_a (equivalently, when convection becomes significant as opposed to diffusion): the increments in J' over the pressure range are factors of $\sim 10^3$ and $\sim 10^{10}$ when $D'_a = 21$ and 664, respectively. Alternatively one can view this as reaching the “high-pressure” limit at lower characteristic pressure when the Damkohler number is small.

V. REVERSIBLE CLUSTERING

The clustering reactions (2)–(5) are now allowed to be reversible, and a nucleation barrier is assumed during the growth sequence. In contrast to the irreversible case, it is not feasible to write the governing equations in dimensionless form, and a dimensional analysis is performed in this section. We explore a limiting case where the monomer concentration is kept constant spatially, in addition to the case where the monomer is produced from the two reactants, as given by Eq. (1).

A. Model parameters

Five clustering steps ($n=5$) are considered for the simulation, and the hexamer, G_6 , is formed irreversibly from reaction (6). In the case when the monomer is formed irreversibly via reaction (1), the rate constant, k_1 , is assumed to be $10^{10} \text{cm}^3 \text{mol}^{-1} \text{s}^{-1}$. Forward rate constants for the clustering in reactions (2)–(6) are all assumed to equal $10^{13} \text{cm}^3 \text{mol}^{-1} \text{s}^{-1}$. The tetramer, G_4 , is assumed to be the critical cluster, below which clusters tend to dissociate and

above which to grow. Accordingly, reverse rate constants are chosen with a constraint that the free energy of formation reaches a maximum value (the free energy barrier height) at the clustering step forming the tetramer. The reverse rate constants k_{-2} , k_{-3} , and k_{-4} are, respectively, assumed to equal 3×10^6 , 2×10^6 , and $1 \times 10^6 \text{s}^{-1}$, allowing slightly decreased reversibility at each step as the clustering proceeds until the critical size. The next reverse rate constant, k_{-5} , is set equal to $1 \times 10^0 \text{s}^{-1}$, which is smaller than k_{-4} by several orders of magnitude, resulting in effectively irreversible growth from G_4 to G_5 . The same values are assumed for species transport properties as in the previous section. The model parameters used for the simulations in the base case are summarized in Table II.

B. Simulation results and discussion

The set of governing equations given in Eqs. (7)–(10), with the boundary conditions, (13) and (14), is solved again by utilizing the computer program PREMIX,⁶ but with non-zero reverse rate constants in this case. For the case where monomer concentration is kept constant, the total mass of the system is not conserved and only Eqs. (9) and (10) constitute the governing conservation equations.

Figure 5 shows calculated distributions of nucleation current and species mole fraction at 1 Torr when the monomer concentration is kept constant at $1 \times 10^{16} \text{cm}^{-3}$. The convection effect is eliminated by setting $u=0$ cm/s. (To maintain the interpretation that the x coordinate also represents time in the flow direction, one can think of this as a very low velocity.) In Fig. 5(a) a transient region is seen to exist up to around $x=0.1$ cm, where a steady-state nucleation current is established. Figure 5(b) shows distributions of cluster mole fractions. All of the mole fractions up to size 5 approach constant values by the end of the transient region. The mole fractions for clusters up to the tetramer are seen to

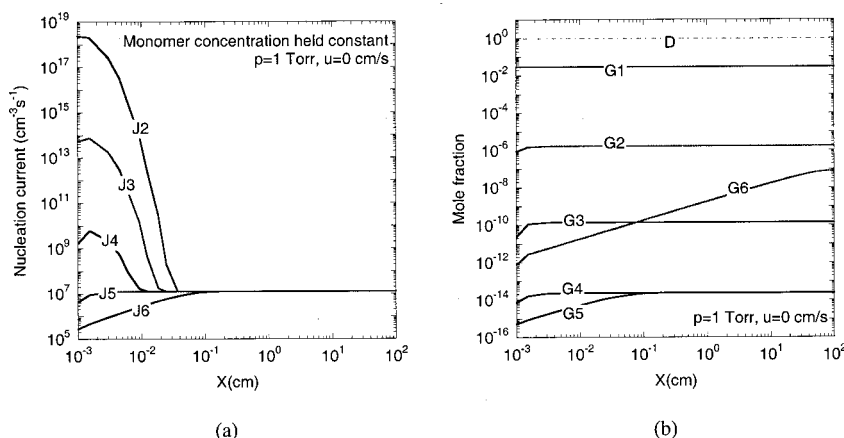


FIG. 5. Distributions of (a) nucleation current and (b) species mole fraction at $p = 1$ Torr. The monomer concentration is kept spatially constant at $1 \times 10^{16} \text{ cm}^{-3}$ and the convective velocity is set to zero.

rapidly approach these constant values, while the mole fraction of the pentamer, being directly coupled to the irreversible formation of particles, continues to climb until it too becomes constant. The mole fraction of particles (G_6) continues to climb in the steady-rate region where the nucleation rate is constant. From the solution to Eq. (10), C_6 here is a quadratic function of x .

With the monomer concentration held spatially constant, the effects of various system parameters are explored in Fig. 6. In Figs. 6(a) and 6(b), respectively, the effects of pressure and convective velocity on the steady-state nucleation current are shown and compared to the case in Fig. 5. Regardless of the variation in the extent of the initial transient region at a different pressure and velocity, all the nucleation currents reach the same value of around $1.2 \times 10^7 \text{ cm}^{-3} \text{ s}^{-1}$ once steady-state nucleation is established. At the higher pressure of 10 Torr in Fig. 6(a), however, steady state is reached earlier compared to the lower pressure case (1 Torr), as diffusion plays a smaller role as pressure increases. Convection also plays a role in delaying the onset of the steady-state region in Fig. 6(b), and the profiles at $u = 10^4 \text{ cm/s}$ are shown to be pushed further toward the downstream boundary. The effect of free energy barrier height on the nucleation rate is shown in Fig. 6(c), with $p = 1$ Torr and $u = 10^4 \text{ cm/s}$. A multiplicative factor to the base-case reverse rate constants, α , is used to adjust the barrier height, so that a higher α represents a higher barrier. As α is decreased by an order of magnitude, the nucleation rate is shown to increase by about three orders of magnitude in the downstream steady-state region. This increment in the nucleation rate can be estimated to be equal to the reduced amount of α , raised to a power equal to the number of steps (three) to the formation of the critical cluster.

Figure 6(d) shows the effect of monomer concentration at $p = 1$ Torr and $u = 10^4 \text{ cm/s}$. The parameter β is used as a multiplicative factor to the base case monomer concentration of $1 \times 10^{16} \text{ cm}^{-3}$. As β is increased by an order of magnitude, the nucleation rate is shown to increase by about five orders of magnitude in the downstream steady-state region. In this reversible clustering case, this increment can be roughly estimated to correspond to the relative increase in β ,

raised to a power equal to the number of clustering steps (five) to *particle*.

In Figs. 7–9, in contrast to the cases shown in Figs. 5 and 6, the monomer concentration is allowed to vary spatially, being produced by the two reactants A and B via reaction (1). The two reactants' concentrations are held constant at $1.7 \times 10^{15} \text{ cm}^{-3}$ at the inlet boundary, and the carrier gas concentration is adjusted according to the total pressure. Figure 7 shows the distributions of nucleation current at $p = 2$ Torr, $u = 10^4 \text{ cm/s}$ and $\alpha = 10^{-1}$. It is evident from this figure that steady-state nucleation is not achieved over the entire domain, because the nucleation currents for clusters below the critical size are nowhere equal to each other. However, the nucleation currents at clustering steps at or beyond the free energy barrier, i.e., J_4 , J_5 , and J_6 , are seen to become close to each other. The differences between two adjacent nucleation currents at the downstream boundary are caused by the diffusion term, $-D_i(d^2C_i/dx^2)$, as seen in Eq. (22). If this term is significant relative to the magnitudes of the nucleation currents, then steady-state nucleation is not possible. Equation (25) indicates that two dimensionless quantities, P' and D'_a , are involved in determining the nucleation rate. Furthermore, if $dC'_A/dx' \geq 0$ and $d^2C'_A/dx'^2 \leq 0$ in Eq. (24), then smaller values of P' and D'_a would result in larger differences between the nucleation currents for adjacent cluster sizes. As the clustering is allowed to be reversible in this case, whereas Eqs. (24) and (25) assume irreversible clustering, the free energy barrier height should also play a role, through the reverse rate constants. We expect that a higher free energy barrier would cause a larger difference between the nucleation currents for adjacent cluster sizes, magnifying the pressure effect.

The effect of varying the total pressure on the nucleation rate is shown in Fig. 8, with $u = 10^4 \text{ cm/s}$ and $\alpha = 10^{-1}$. In Fig. 8(a) a larger pressure sensitivity is predicted at lower pressure, which is caused by the fact that the diffusion coefficient is inversely proportional to pressure. The nucleation rate is seen to increase by a factor of almost five for an increase in pressure from 0.1 to 2 Torr, whereas it barely changes thereafter even for the much larger pressure increase

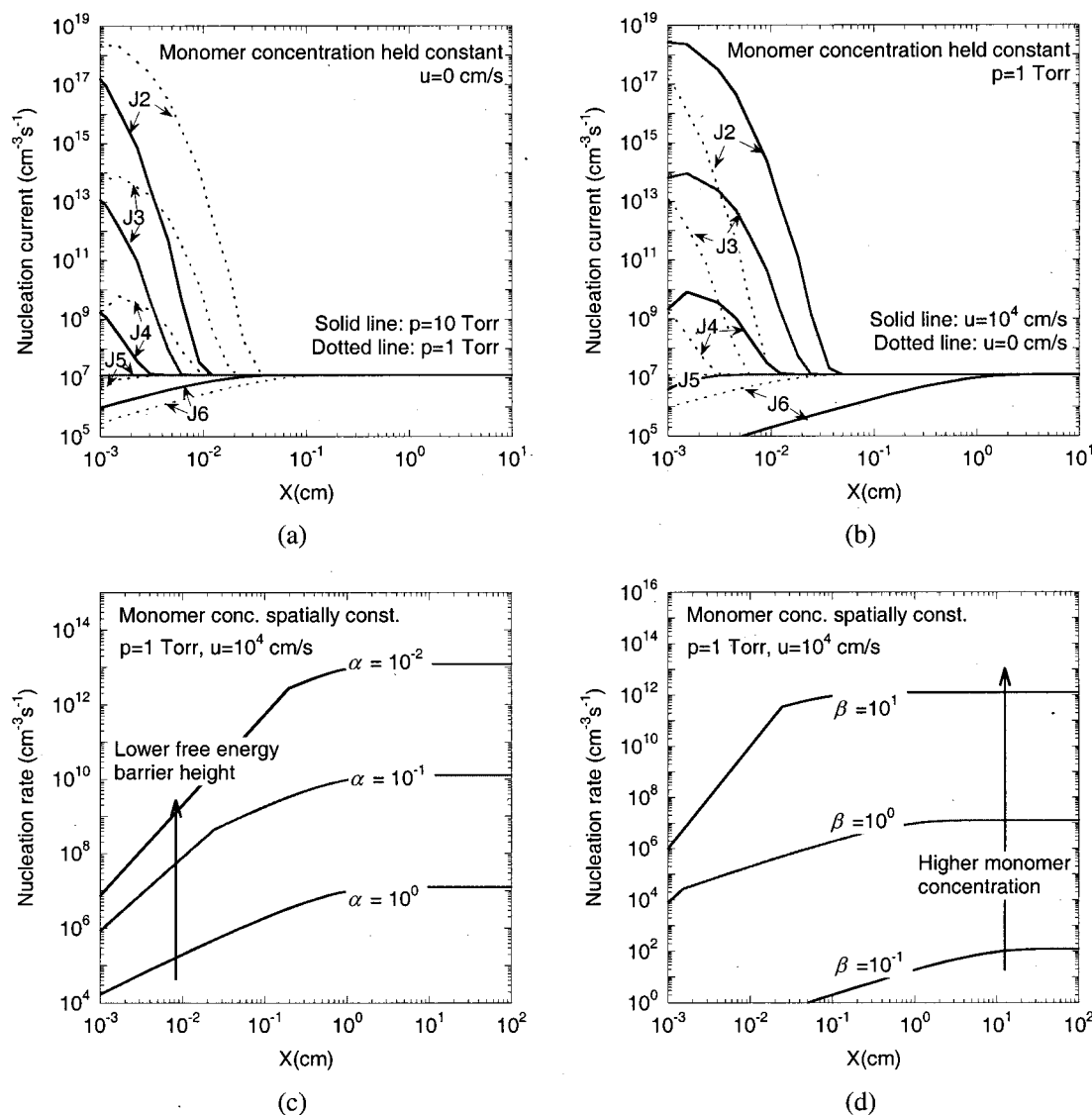


FIG. 6. Effects of system parameters on nucleation rate with the monomer concentration kept spatially constant. In (a)–(c) the monomer concentration equals $1 \times 10^{16} \text{ cm}^{-3}$. Distributions of nucleation current: (a) effect of pressure with $u=0 \text{ cm/s}$; and (b) effect of residence time with $p=1 \text{ Torr}$. Distributions of nucleation rate: (c) Effect of free energy barrier height with $p=10 \text{ Torr}$ and $u=10^4 \text{ cm/s}$. A multiplicative factor α is applied to the base-case reverse rate constants; (d) effect of monomer concentration at $p=10 \text{ Torr}$, $u=10^4 \text{ cm/s}$ and $\alpha=10^{-2}$. A multiplicative factor β is applied to the base case monomer concentration.

from 2 to 10^3 Torr . As seen from the dimensionless analysis in Figs. 2–4, the nucleation rate becomes more sensitive to pressure at lower pressures (P'), at lower reactant concentrations ($C'_{A,0}$), at lower monomer production rates (R'^{-1}), and at longer residence times (D'_a).

Compared to the case in Fig. 8(a), a larger pressure sensitivity is found in Fig. 8(b), in which several parameters affecting the key dimensionless quantities have been varied. A multiplicative factor γ is applied to the base case rate constant k_1 , $1 \times 10^{10} \text{ cm}^3 \text{ mol}^{-1} \text{ s}^{-1}$. The assumption of a smaller value of u (equivalently, a larger value of D'_a) and a smaller value of γ (equivalently, a smaller value of R'^{-1}) results in an increase in the nucleation rate by about two orders of magnitude for the pressure change from 0.1 to 2 Torr. Had a smaller value of α not been assumed here, solely

for computational reasons, the pressure sensitivity in the low-pressure regime would be even greater.

The effect of the monomer production rate was explored by varying γ , as shown in Fig. 9. A higher monomer production rate causes a higher nucleation rate in general. The nucleation rate is seen to increase by more than three orders of magnitude for a change of γ from 10^{-1} to 10^0 , but not as much for further increase in γ from 10^0 to 10^1 . This reduced sensitivity of the nucleation rate to the monomer production rate at higher values of γ is mainly attributable to reactant depletion.

VI. CONCLUSIONS

An analytical and numerical study was conducted to investigate the effect of pressure on gas phase nucleation. A

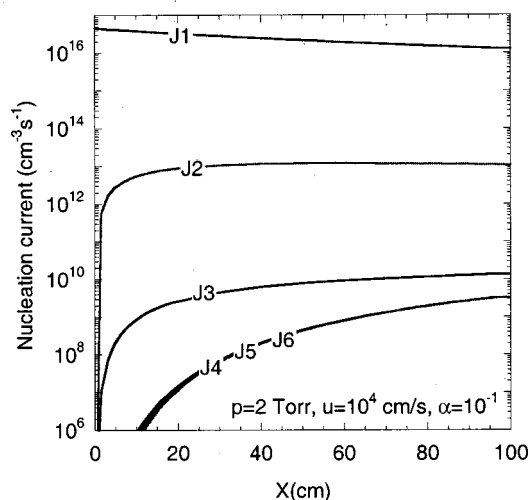


FIG. 7. Distributions of nucleation current at $p=2$ Torr, $u=10^4$ cm/s and $\alpha=10^{-1}$.

sequence of chemical clustering reactions was assumed to model a generic self-clustering mechanism leading to particle formation. Species conservation equations were formulated for a steady-state, isothermal, isobaric, one-dimensional, plug flow reactor, considering species transport by convection and diffusion. From examination of the governing equations, the conditions of validity for the approximation of a steady-state nucleation current were examined. Two types of simulations were conducted according to whether or not the clustering reactions were assumed to be reversible. Based on the results, the major conclusions can be summarized as follows:

- (i) In the case of reversible clustering, if one assumes that the monomer concentration is constant, then the presence of a rate-limiting bottleneck leads to the es-

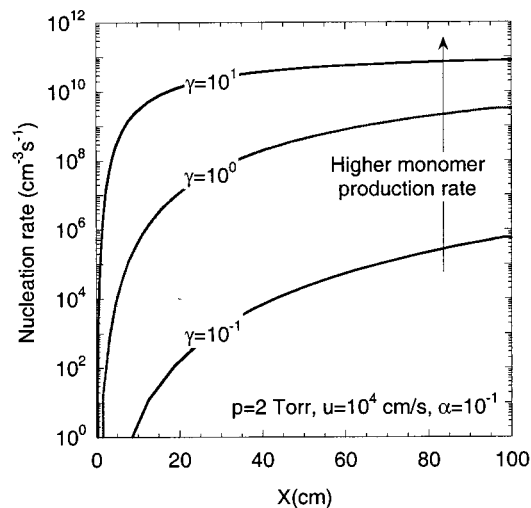


FIG. 9. Effects of the monomer production rate constant, k_1 , on nucleation rate at a convective velocity of $u=10^4$ cm/s and $p=2$ Torr.

tablishment of a steady-state nucleation current, where all the nucleation currents are equal to each other and the nucleation rate is independent of total pressure;

- (ii) when the monomer concentration is allowed to vary, then, regardless of reaction reversibility, species diffusion causes the nucleation rate to become a sensitive function of total pressure for sufficiently low pressures. In this regime, steady-state nucleation is not possible;
- (iii) the nucleation rate is more sensitive to total pressure at lower pressures, lower reactant concentrations, lower monomer production rates, longer residence times, and higher free energy barriers to nucleation.

These results indicate that to minimize particle genera-

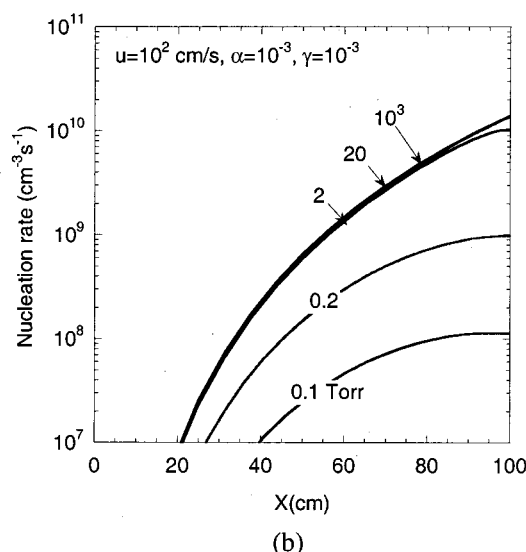
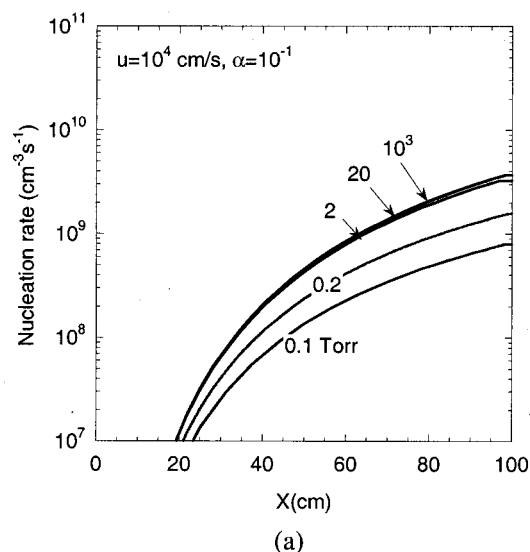


FIG. 8. Distributions of the nucleation rate with varying pressure at: (a) $u=10^4$ cm/s and $\alpha=10^{-3}$; (b) $u=10^2$ cm/s, $\alpha=10^{-3}$ and $\gamma=10^{-3}$, where γ is a multiplicative factor applied to the base case value of k_1 .

tion in CVD reactors one should operate, all else being equal, at lower absolute pressure in the reactor while maintaining a constant partial pressure of the reactants. For example, referring to Fig. 2, one could increase the reactant concentration by a factor of four (from 0.5 to 2) while maintaining the same rate of particle generation by decreasing the total pressure by a factor of 10. The increased reactant concentration would presumably lead to increased film deposition rates, assuming that the rate constants for pertinent chemical reactions are independent of pressure.

ACKNOWLEDGMENTS

This work was partially supported by NSF Grant No. CTS-9909563 and by the Minnesota Supercomputing Institute.

- ¹S. L. Girshick, M. T. Swihart, S.-M. Suh, M. R. Mahajan, and S. Nijhawan, *J. Electrochem. Soc.* **147**, 2303 (2000).
- ²S. Nijhawan, Ph.D. dissertation, University of Minnesota (1999).
- ³T. Kim, S.-M. Suh, S. L. Girshick, M. R. Zachariah, P. H. McMurry, R. M. Rassel, Z. Shen, and S. A. Campbell, *J. Vac. Sci. Technol. A* (to be published).
- ⁴M. Liehr and S. A. Cohen, *Appl. Phys. Lett.* **60**, 198 (1992).
- ⁵S.-M. Suh, M. R. Zachariah, and S. L. Girshick, *J. Aerosol Sci.* (to be published).
- ⁶R. J. Kee, J. F. Grcar, M. D. Smooke, and J. A. Miller, Sandia National Laboratories Report SAND85-8240, Albuquerque, NM (1985).
- ⁷R. J. Kee, F. M. Rupley, E. Meeks, and J. A. Miller, Sandia National Laboratories Report SAND96-8216, Albuquerque, NM (1996).
- ⁸A. E. Lutz, R. J. Kee, and J. A. Miller, Sandia National Laboratories Report SAND87-8248, Albuquerque, NM (1988).
- ⁹M. R. Zachariah and W. Tsang, *Aerosol. Sci. Technol.* **725**, 1560 (1993).
- ¹⁰M. R. Zachariah and W. Tsang, *J. Phys. Chem.* **99**, 5308 (1995).